Dislocation Arrays and the Bauschinger Effect in Copper 9 at. % Aluminum Bicrystals

By

Satoshi HASHIMOTO* and Sei MIURA*

(Received June 27, 1985)

Abstract

Dislocation arrays in lightly deformed Cu-9 at.% Al bicrystals, whose component crystals have a crystallographic mirror symmetry with respect to the grain boundary, are observed by the etch-pitting technique. Then, the influence of the grain boundary on the Bauschinger effect is discussed. It is shown that the induced secondary slips near the boundary can be explained quantitatively in terms of stress concentration due to the piled-up dislocations of adjacent crystal. Some of them can be also explained by the microscopic incompatibility owing to the mismatch of primary slip bands in each component crystal at the boundary. From the observations of reversed bicrystals, it becomes evident that the induced secondary dislocations near the boundary, which exist mostly by forming double ended pile-ups between the primary slip bands, are unstable against reverse stress. Namely, most of them are annihilated in the first stage of reverse stressing, and are subsequently recovered by a further reverse stress. It is pointed out that although primary dislocations near the boundary can move even a small reverse stress backwards by the aid of high back stress on dislocations because of the latent hardening by multiple slips and pile-up dislocations, the mean free path of the primary dislocations is thought to be small due to the interference of secondary dislocations. Consequently, the Bauschinger effect in a multiple slip layer is presumably smaller than that in the center of each component crystal.

1. Introduction

The contribution of grain boundaries to the Bauschinger effect is an important factor since the metallic materials used in practice are mainly polycrystalline aggregates. In spite of the conflicting evidence of Sachs and Shoji[1] of a large Bauschinger effect in single crystals of alpha-brass, the effect could be explained by the development of a residual intergranular stress system assisting a reverse stress, and arising from the heterogeneous deformation pattern of an aggregate of anisotropic grains[2,3].

Recently, Buckley and Entwistle[4] have investigated the magnitude of the Bauschinger effect in both single and poly-crystals of aluminium. They demonstrated

* Department of Engineering Science, Faculty of Engineering, Kyoto University, Kyoto-606, Japan

that, in single crystals, stressing in easy glide results in large Bauschinger strains which are proportional to the amount of prestrain, and do not increase significantly beyond this stage. The effect of polycrystals is then smaller than that of single crystals. The trend of the results of the Bauschinger effect can be generally interpreted as favouring the possibility of a long-range reverse slip of dislocations in easy glide. It also throws light on the behaviour of work hardening of fcc metal single crystals and polycrystals. While Gokyu et al.[5] have reported that the Bauschinger effect is large for finger grain-size, and that with an increasing prestrain the grain size dependence of alpha-brass and copper becomes smaller, except in the case of mild-steel. They explained the results of grain-size dependence, taking into account the concept of the so-called Heyn stress[2] which is postulated to be attributable to the residual internal stress due to the difference of the relative ease of deformation in each grain. They also suggested that the formation of dislocation cell structure with increasing strain leads to a subsequent small dependence. However, the discrepancy between the magnitude of the effect of single crystals and polycrystals having different grain sizes is as yet unsolved.

The difficulty of the problem arises from the complicated interaction between crystals due to the existence of grain boundaries. A logical approach evaluating the interaction between adjacent grains is to examine both the mechanical behaviour and the dislocation arrays by employing simple bicrystals. Takamura and Miura[6] found a decrease of indentation hardness near the grain boundary region, and a slight increase in the center of grain in a second compression of α-brass bicrystal after primary extension. They suggested that a large part of the grain boundary hardening is due to the piled-up dislocations against the boundary. They also suggested the observed change in hardness is closely connected with the Bauschinger effect.

The purpose of the present paper is to report some preliminary etch-pit observations of dislocation arrays near the grain boundary of lightly deformed symmetric Cu-9 at. % Al alloy bicrystals, and then to comment on the influence of the grain boundary on the Bauschinger effect.

Until, now, numerous experimental studies of bicrystals have been reported[7], but there have been few results reported about the direct observations of dislocation distributions of fcc metal bicrystals of controlled direction by employing an etch pitting technique. However, extensive etch-pit work on Fe-3% Si bicrystals was performed by Hook and Hirch[8-10]. Therefore, the observations of microscopic slip at the boundary will also supply additional informationon the problem of the effect of the grain boundary on the mechanical behaviour of fcc metal bicrystals.

2. Experimental Procedure

The materials used in this study were Cu-9.2 at. % Al alloy. Oriental bicrystals were grown from the seed in split graphite moulds with two seed cavities by the Bridgman method under a dynamic vacuum of less than 10^{-5} torr. The isoaxial bicrystals grown were of rectangular cross section ($4.5 \times 19\ mm^2$), had the growth direction and tensile axis [431] and a pair of surfaces parallel to the $(1\bar{1}\bar{1})$ plane within $\pm 3°$ determined from back-reflection Laue X-ray diffraction pattern. The bicrystal geometry, the reference axes and the stereographic projection of primary slip plane and primary Burgers vector in each component crystal are shown in Figs. 1 and 2 respectively.

The component crystals A and B have a crystallographic mirror symmetry with respect to the grain boundary. Etch pitting was undertaken on the $(1\bar{1}\bar{1})$ plane.

The crystals were then shaped using a spark cutting machine. After shaping, the specimens were cyclic-annealed for about a hundred hours between 1 040–750 °C by periodically switching on and off the current of a heating furnace under a dynamic vacuum of less than 10^{-4} torr. Consequently, the specimen had dislocation densities ranging from 1×10^5 to $5 \times 10^5/cm^2$, and had subgrain diameters ranging from 1.0 to 0.5 mm.

The etching solution used in the present experiment was mainly Young's type[11], because this etchant has a rather larger permissible limit of disorientation from the

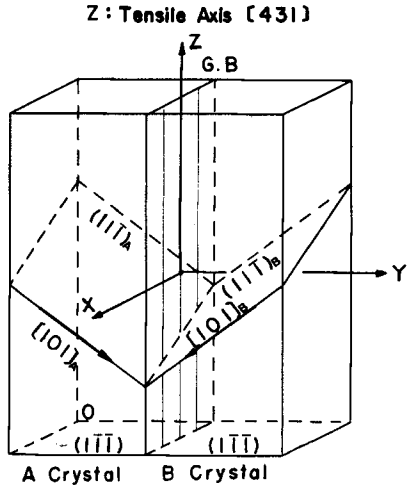

Fig. 1. Schematic representation of isoaxial symmetric bicrystal used. Tensile axis Z is [431] and parallel to the boundary plane X-Z. Primary slip system $(11\bar{1})$ $[101]$ in each crystal is also indicated.

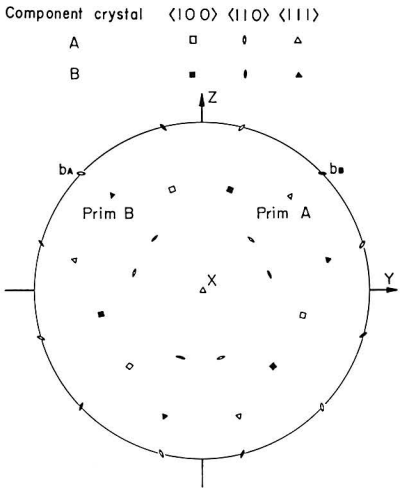

Fig. 2. Stereographic projection of crystallographic orientation of bicrystal. Primary slip system of each component crystal is indicated.

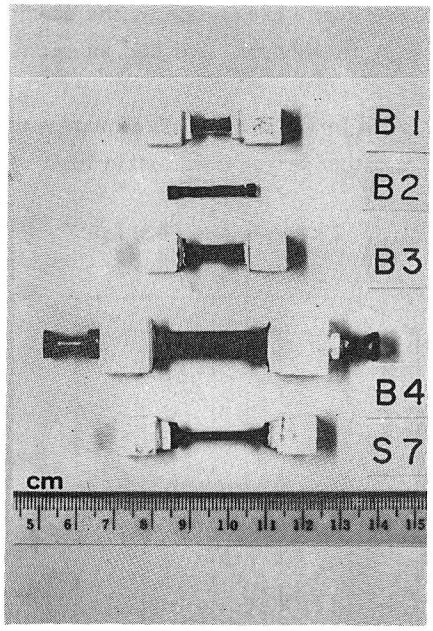

Fig. 3. Shape of specimens used.

{111} plane for revealing the etch pit than that of Livingston's type[12]. The etchant has the following composition: 3 cc of hytrobromic acid, 75 g of ferric chloride($FeCl_3$ $6H_2O$), 80 cc of hydrochloric acid and 100 cc of distilled water.

The bicrystal and single crystals were deformed at a cross head speed of 0.05

mm/min in an Instron type testing machine at room temperature. The final shapes of the specimens are presented in Fig. 3. Bicrystal specimens B1 and B3 for the tension-compression test, B2 for the four-point bending test, and B4 and the single crystal specimen S7 having the same crystallographic orientations as a component crystal for an undirectional tensile test are shown in the figure. The bicrystals B1, B3, B4 and the component single crystals S7, S8 had gauge lengths of 7, 12, 23 and 17 mm, respectively. All the specimens had the thickness of 3.5-3.0 mm. The grain boundary of each specimen was almost parallel to the tensile direction [431] and divided into equal parts in width. The bicrystal specimen B2 was stressed reversely by applying a pure bending moment, using a four-point bending jig. Up to the stress just beyond yielding by a four-point bending test, the dislocation behaviour near the surface is almost identical to that by the simple tension or compression test from the results of etch pit observations of copper by Young[13,14].

3. Results

3.1. Dislocation arrays of unidirectionally deformed bicrystals

The normal stress versus strain curves of component single crystals and bicrystals are shown in Fig. 4. The values for the critical resolved shear stress, τ_y, of both single and bi-crystals are also shown in Table 1. In this table, the values of specimens named S1, S2 and S3 were taken from the results of the component single crystals for reference. It was found that the mean value of critical stresses for bicrystals is slightly larger than that for component single crystals. It was also found

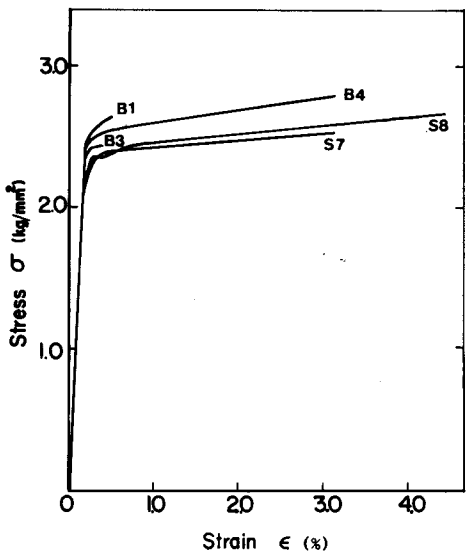

Fig. 4. Normal stress-strain curves ot single and bi-crystals.

Table 1. Critical resolved shear stress, τ_y, of single crystals and bicrystals.

Specimen	No.	τ_y (kg/mm²)	Deformation
Single Crystal	S 7	1.12	Tension
	S 8	1.10	〃
	S 1	1.10	Compression
	S 2	1.00	〃
	S 3	1.10	〃
Bicrystal	B 1	1.22	Compression
	B 3	1.14	Tension
	B 4	1.19	〃

that the coefficient of work hardening of the former is also slightly larger, as can be understood in the figure and table.

The surface slip markings which appeared on the $(1\bar{1}\bar{1})$ plane after straining just past yielding are shown in Fig. 5. Traces on this observation surface for slip planes are also indicated. It was found that even at the very beginning of plastic deformation, critical and conjugate slip systems were activated in the vicinity of the boundary. Considering the geometry of the component crystals, slip markings aris-

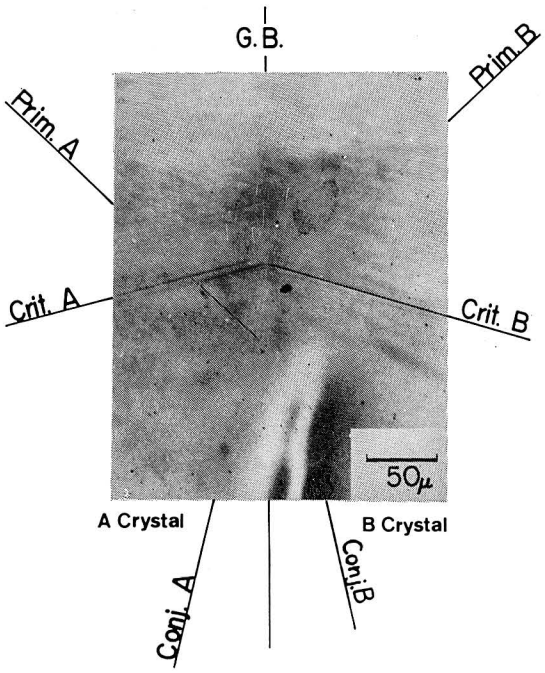

Fig. 5. Slip lines on $(1\bar{1}\bar{1})$ surface in the vicinity of grain boundary just after yielding in specimen B5.

ing from the operation of primary slip system $(1\bar{1}\bar{1})$ [101] are never revealed in the true $(1\bar{1}\bar{1})$ plane. However, the observation surface of the specimen deviated by a little angle of $\simeq 3°$ from $(1\bar{1}\bar{1})$ so that faint primary markings were observed in the present crystal. In the component crystal A, a much more well-defined primary

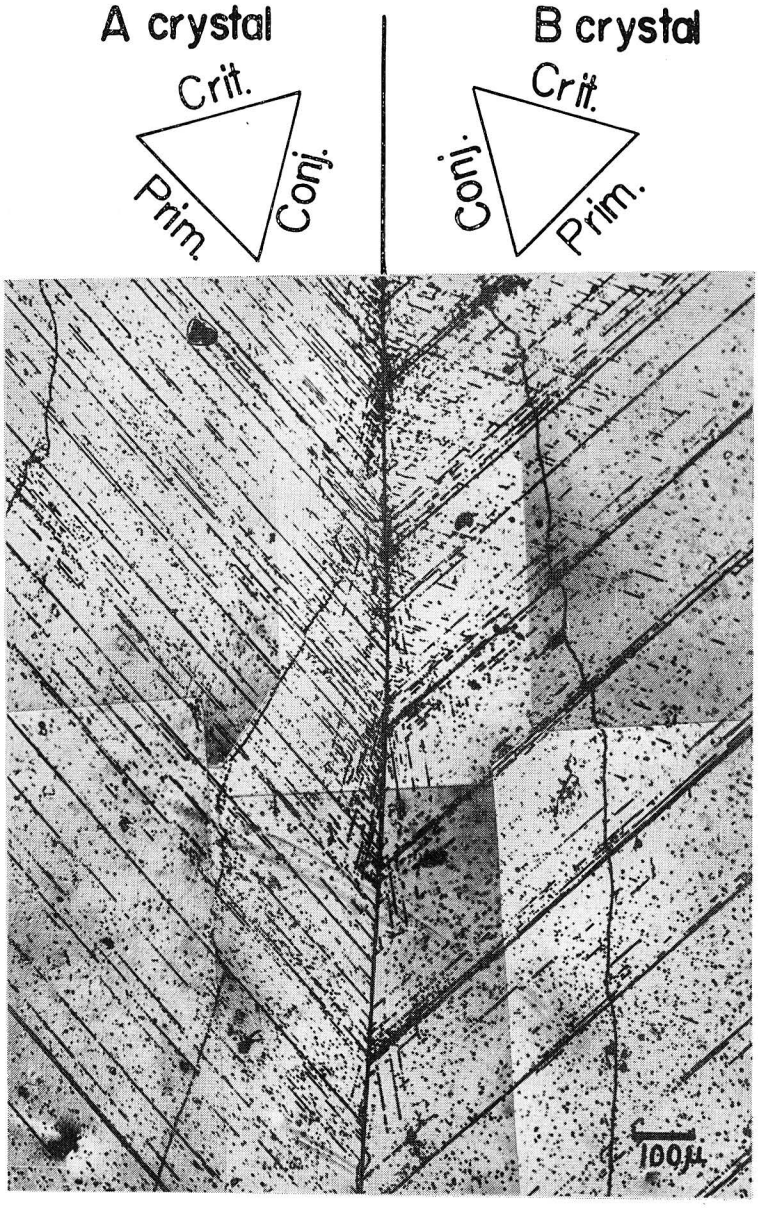

Fig. 6. Dislocation etch-pit distributions after straining just past yield in specimen B1.

marking was observed only near the boundary. This suggests the operation of the primary coplanar slip system. Thus, it is concluded that the various dislocation sources of slip systems other than the primary system operate near the boundary, even by a straining just the yield. This symmetric bicrystal can deform on the two primary slip systems alone, one in each component, and still maintain continuity at the grain boundary plane. The reason is that the plastic strain components are equal in each component crystal from the view point of macroscopic plasticity, neglecting the inhomogeneities on a microscopic scale[15,16]. This will be discussed in the following section 4. 1. 1.

Dislocation distibutions obtained by an etch pitting technique are shown in Fig. 6. The pattern of the primary slip in each component is not quite symmetrical with respect to the grain boundary. Induced secondary slip systems were visible at the grain boundary. Figure 7 shows the variation of the feature of dislocation distributions neare the boundary of an identical area with an increasing tensile strain. Macroscopic configurations of dislocations for the component single crystal and the bicrystal extended by a strain of 3.0% are presented to compare the nature

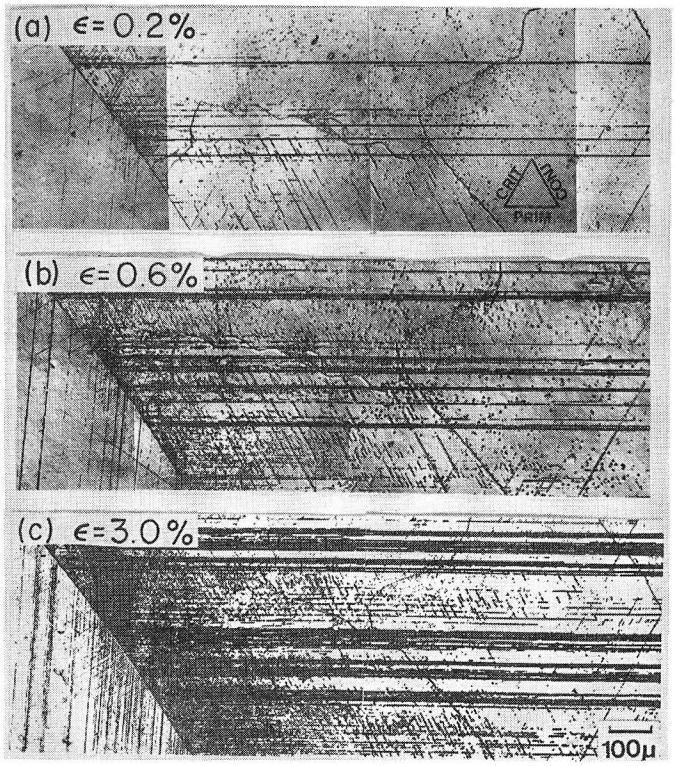

Fig. 7. Change of dislocation structure near the grain boundary with increasing tensile strain in specimen B4.

of deformation for both crystals, as shown in Fig. 8 (a) and (b) respectively. In these photographs for bicrystals, somewhat ill-defined etch pits in the adjacent crystal are caused by the disorientation from the $(1\bar{1}\bar{1})$ plane. This is because the maximum angular deviation of {111} from the plane of the surface which still permits the revealing of etch pits is smaller than 2.5°.

In regions along the grain boundary where the density of slip was high, complex clusters composed of short primary and secondary slips were observed. These were formed predominantly at the head of 'strong' primary slip bands of adjacent crystal. The secondary slips, occurring at the boundary, extended rather uniformly with an increasing strain over 0.2 to 0.3 mm into the component crystal after the strain of 3.0%. In this region, much higher etch-pit density zones were formed along the direction of the primary slip of the adjacent crystal. This suggests that the high stress concentration caused by the piled-up dislocations of adjacent crystals promotes the activation of additional slips near the boundary. The operation of the

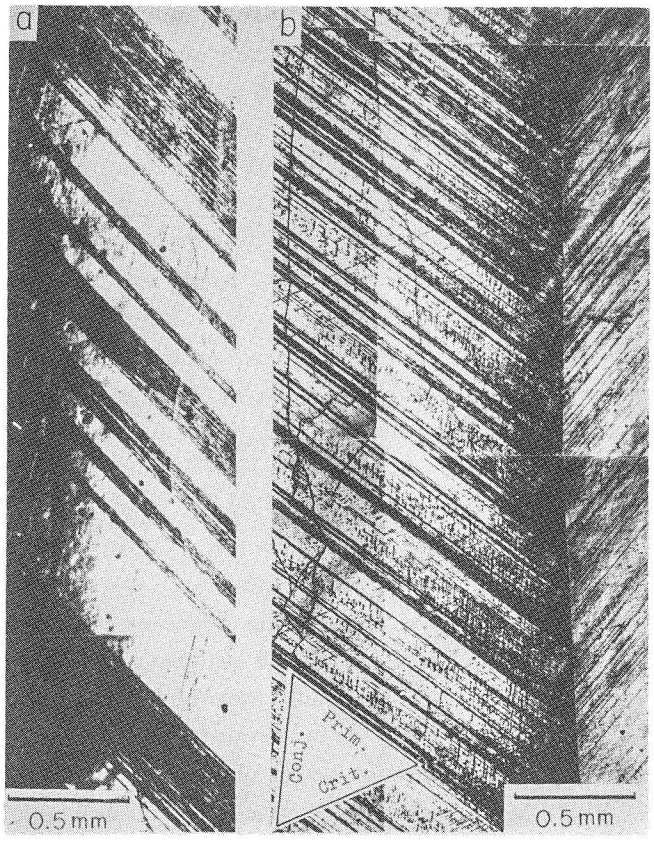

Fig. 8. Macroscopic dislocation configurations after a tensile strain of 3% in single crystal S7 (a) and bicrystal B4 (b).

conjugate slip system between the primary bands were visible, and this extended over 2.5 to 3.0 mm from the boundary after the strain of 3.0%.

The mean width of the primary bands of bicrystal was far narrower than that of single crystal. The bands were distributed at almost equal spaces in the entire region of the gauge length. In a single crystal of the present alloy, one or several narrow slips are generated as nuclei of bands after yielding. Then, these extend the width of the bands with an increasing strain, the behaviour of which is similar to that of the so-called Lüders band. It appears, however, that in the bicrystal, many primary slips are formed simultaneously at yielding, and that these are distributed uniformly in the entire region of the gauge length. This effect due to the existence of the grain boundary is the first occasion we know of.

3.2. Dislocation behaviour near the grain boundary under reverse stressing

3.2.1. Four point bending specimen B2

The specimen was successively stressed until the first dislocation multiplication occurred by using a four-point bending jig, setting the observation surface down, i.e. tensile prestress was applied to the observation surface's side. The change of the loading direction was attained simply by setting the surface upward. No attempt was made to measure the strain during the course of the experiment. Reverse stressings by compression is terms of the reverse stress ratio τ_{rc}/τ_{pt} of 0.5, 0.75, and 1.5, and then again reverse stressings by tensions of 0.5, 0.75, and 1.0, were performed in the experiment on the specimen. Here, τ_{rc} and τ_{rt} are the compressive and tensile reverse stresses, τ_{pt} and τ_{pc}, the tensile and compressive pre-stress, and in the definition $\tau_{pc}=1.5\tau_{pt}$.

Figures 9, 10 and 11 show the dislocation behaviours near the grain boundary under the reverse stressings. The back motion of dislocations already took place even after the reverse stressing of the ratio 0.5. This behaviour can be seen in the dislocation groups A, C and D in Fig. 9. The back motion taking place during the next reverse stressing and the annihilation of dislocations were frequently observed in the reverse stressings of 0.5 and 0.75. This can be seen, for example, in groups B, E, F and G.

Double ended pile-ups, B, sited near the boundary after prestressing were almost completely annihilated during the reverse loading, as is seen from the double etch-pit micrograph of Fig. 9 (b). A similar type of annihilation of double ended pile-ups, E, was observed in Fig. 10. It is considered that these dislocation groups near the boundary have a multiplication source of the Frank-Read type inside the crystal surface. These had no barriers such as secondary dislocations induced by the concentration of piled-up dislocations of adjacent crystal. As a result, these will be able to be annihilated during a reverse loading by a mutual encountering of disloca-

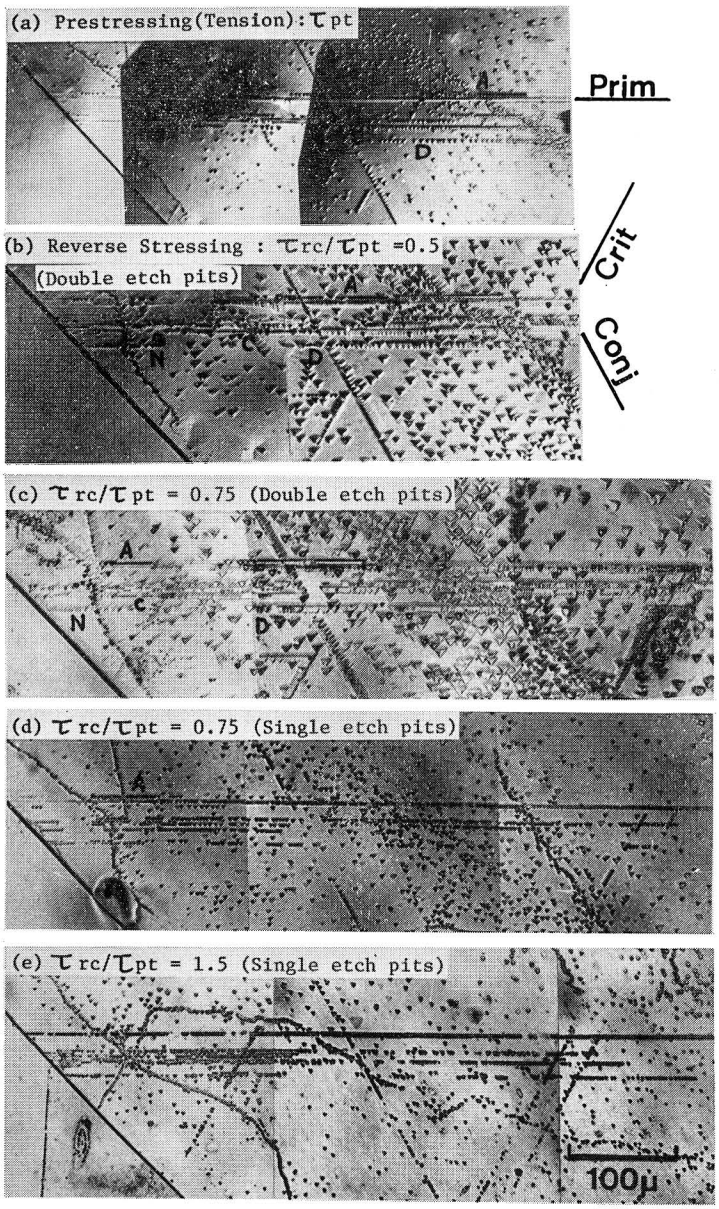

Fig. 9. Behaviour of dislocations near the grain boundary under reverse stressings in specimen B2.

tions of the opposite sign. However, if some dislocations on one side of the double ended pile-ups were impeded by some barriers during back motion and were not able to travel back across them completely, the dislocations would not be annihilated completely, and some dislocations would remain. It is natural to consider that this

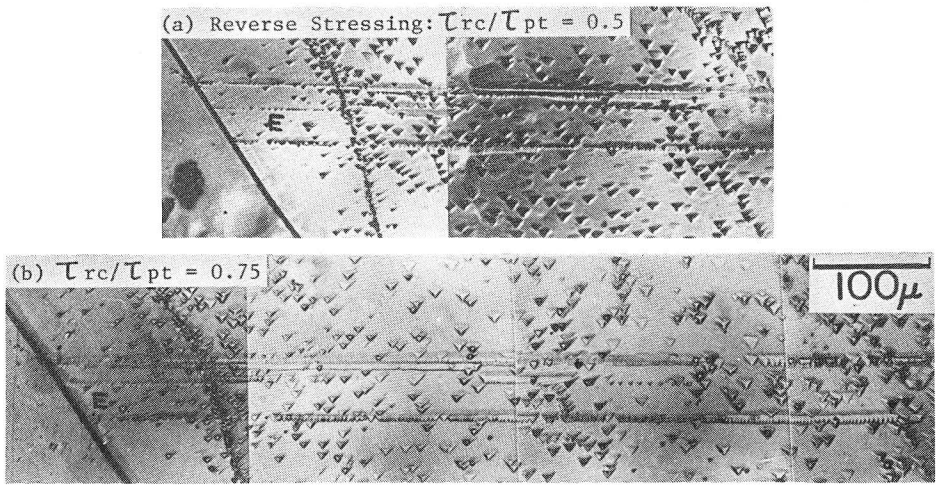

Fig. 10. Annihilation of dislocation pile-ups E during reverse stressing in specimen B2.

must frequently occur near the boundary, due to many secondary slips induced by the stress concentration of adjacent slips. It seems that behaviour of this type would occur commonly, as can be understood from the results of Fig. 9 (d) where the most piled-up dislocations against boundary after prestressing were not annihilated thoroughly, and had a dislocation vacant region behind the row. The two sequences of reverse motion of piled-up dislocattions, whose multiplication source is near the boundary, are indicated schematically in Fig. 12.

In the reverse deformation of bicrystal, the secondary dislocations near the boundary play a very important role in preventing a back motion of primary dislocations. However some stable distributions of dislocations, such as dipole or attractive junctions with the forest dislocations, also contribute to the interference of the reverse motion of primary dislocations. Thus, it may be considered that in bicrystal the mean distance of reverse motion of dislocations is smaller than that in single crystal because of the secondary dislocations acting as a barrier.

The specimen was them stressed to $1.5\tau_{pt}$. No significant change in dislocation distributions was observed, though the dislocation density became slightly higher (Fig. 9 (e)). Poor mobility of dislocations during the subsequent reverse stressings of 0.5, 0.75 and $1.0\tau_{pc}$ was observed. This may be caused by the cyclic work hardening due to the formation of dipoles or some attractive junctions with forest dislocations during the reverse loading which are stable against reverse loading.

Striking evidence of the mutual annihilation of dislocations which formed double ended pile-ups is presented in Figs. 13 and 14. Point H in these figures will serve as a reference point of the identical position. It can be seen that the left-hand pile-ups are dark and the right-hand ones are light. This strongly suggests that

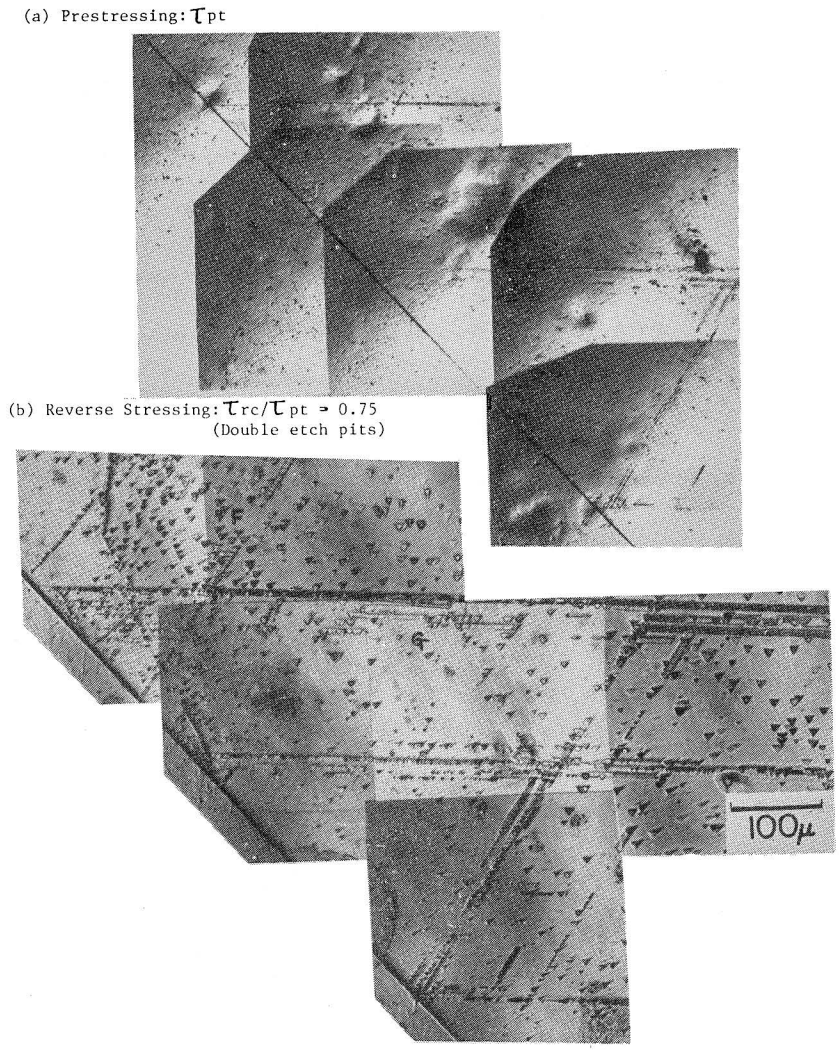

Fig. 11. Behaviour of dislocations near the grain boundary under reverse stressing in specimen B2.

these pile-ups correspond to positive and negative edge dislocations. This manifestation is in agreement with the nature of etch pits using Livingston's etchant[17]. These pile-ups were completely collapsed by the mutual annihilation of dislocations of the opposite sign, as is seen in the series of photographs of Fig. 14. It should be emphasized that (these types of pile-ups are) much more unstable against reverse loading, since no significant change of other dislocation distributions was observed.

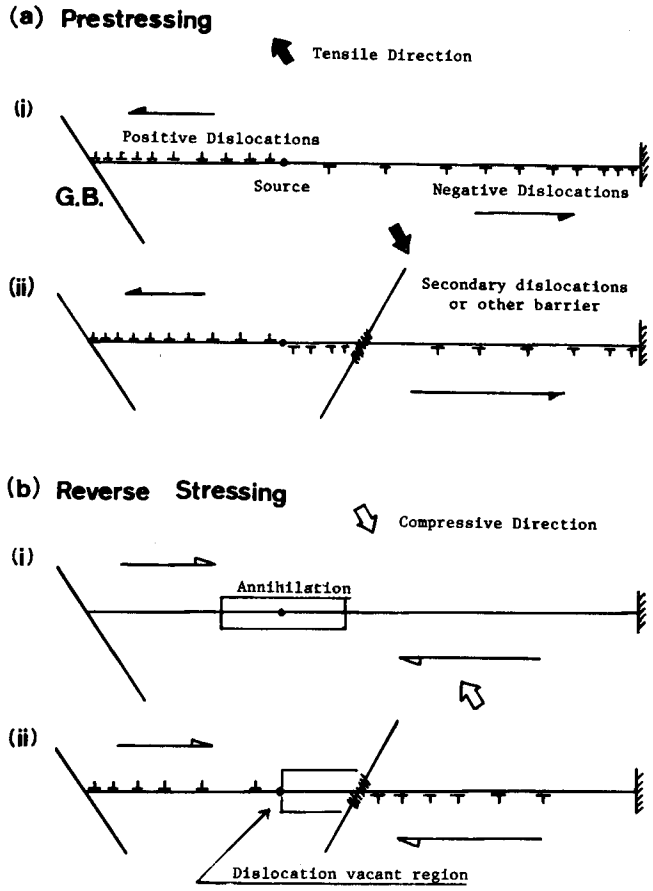

Fig. 12. Schematic representation showing behaviour of pile-up dislocations near the boundary during reverse stressing. Pile-ups having no barrier can move backward and be annihilated completely as shown in (a) (i) and (b) (i), but if any barrier impinges against pile-ups during pre-stressing, (a) (ii), all of the dislocations cannot travel back completely to the source and some of them would remain, (b) (ii).

3.2.2. Tension-compression specimen B1 and B3

Specimen B1 was initially stressed in compression till yielding was recognized on a load-time chart and then unloaded. After etch-pitting to observe the dislocation arrays, the specimen was subjected in tension to the reverse stress ratios of 3/4 and then 1. The changes of dislocation arrays were observed under each reverse stressing. The changes of the feature of dislocation arrays near the boundary are shown in Fig. 15. The number of short dislocation groups which may be generated by the stress concentration of primary pile-up dislocations of adjacent crystal was remarkable after the pre-stressing (Fig. 15 (a)). After the first reverse stressing

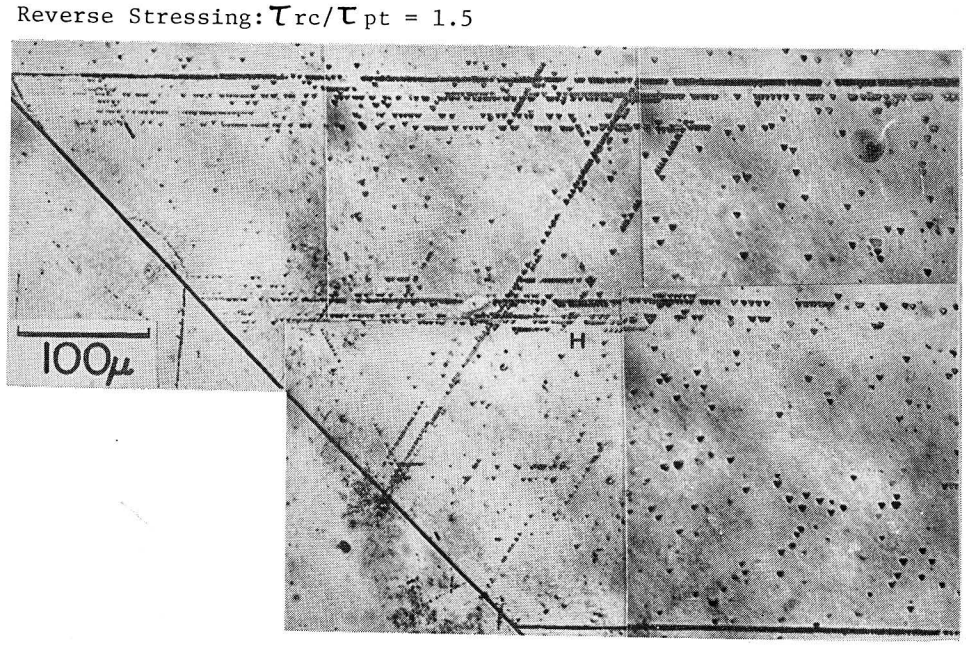

Fig. 13. Dislocation distributions after reverse stressing in the same region in Fig. 11. Double ended pile-ups near a reference point H disappeared during the subsequent reverse stressing as shown in the next figure.

($\tau_r = 3/4\,\tau_p$), these arrays almost disappeared, though very short secondary dislocations at the cross-points with primary dislocations remained. (Fig. 15 (b).) Hence, it is considered that these dislocations are easily collapsed by a mutual annihilation of dislocations of opposite sign, since each group of the dislocations has its source in between bands of primary dislocations. The dislocations emitted are then not permitted to slip long range distances because of the interference by primary dislocations. It becomes evident that these short dislocation groups are much unstable against reverse loading. The detailed behaviour of dislocations in the primary slip bands composed of densely aligned dislocations was not observed closely. However, no significant change in their distributions was observed from a macroscopic view point, though a back motion of individual dislocations would take place in the bands.

After the following reverse stressing, the nature of dislocation distributions and dislocation density developed in a way similar to that after initial stressing, i. e. most of the additional dislocations near the boundary recovered at the same portions, as can be seen in Fig. 15. From the results, it can be concluded that during a subsequent reverse loading the same sources will emit dislocations of opposite sign, and these dislocations will again pile up against primary dislocations. The occur-

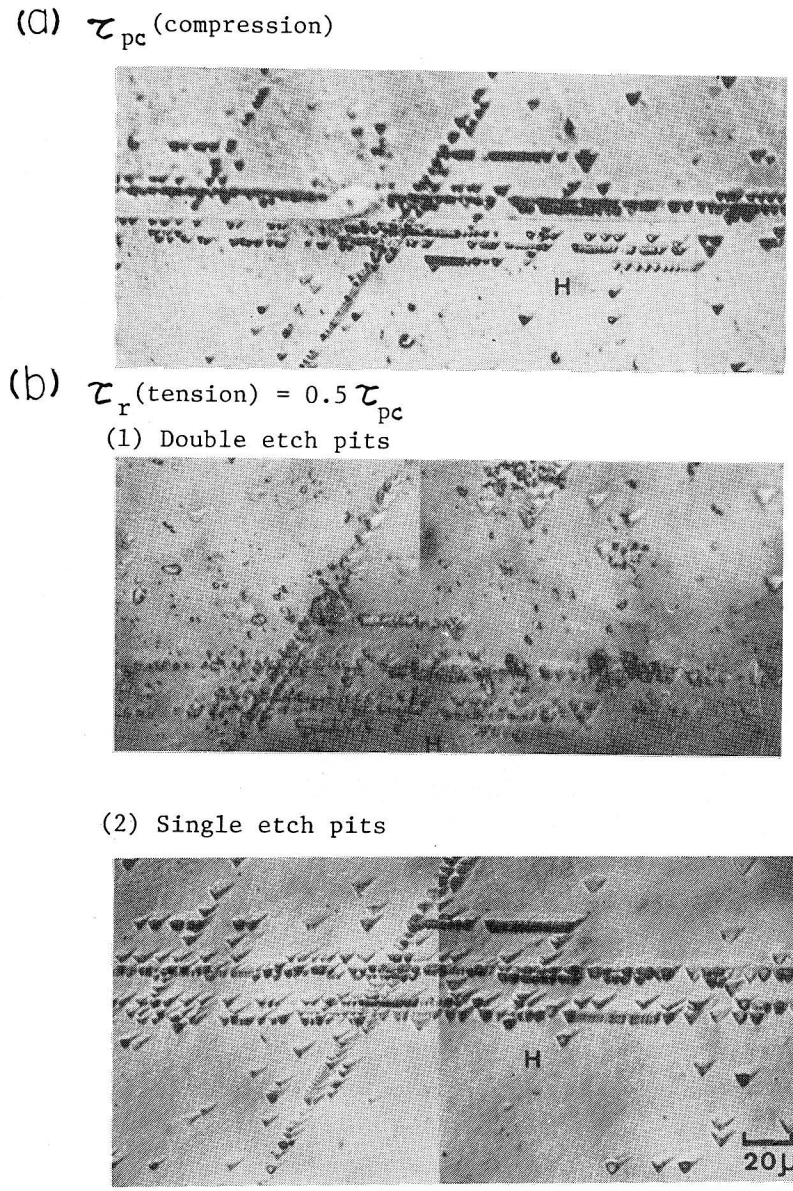

Fig. 14. Annihilation of double ended pile-ups H during reverse stressing.

rence of the annihilation of the dislocations as well as the back motion of primary pile-up dislocations will promote a weakening of the grain boundary strength in the early stage of reverse loading, and must be closely connected with the Bauschinger effect in bicrystal.

Figure 16 shows the dislocation distributions after yielding in specimen B3.

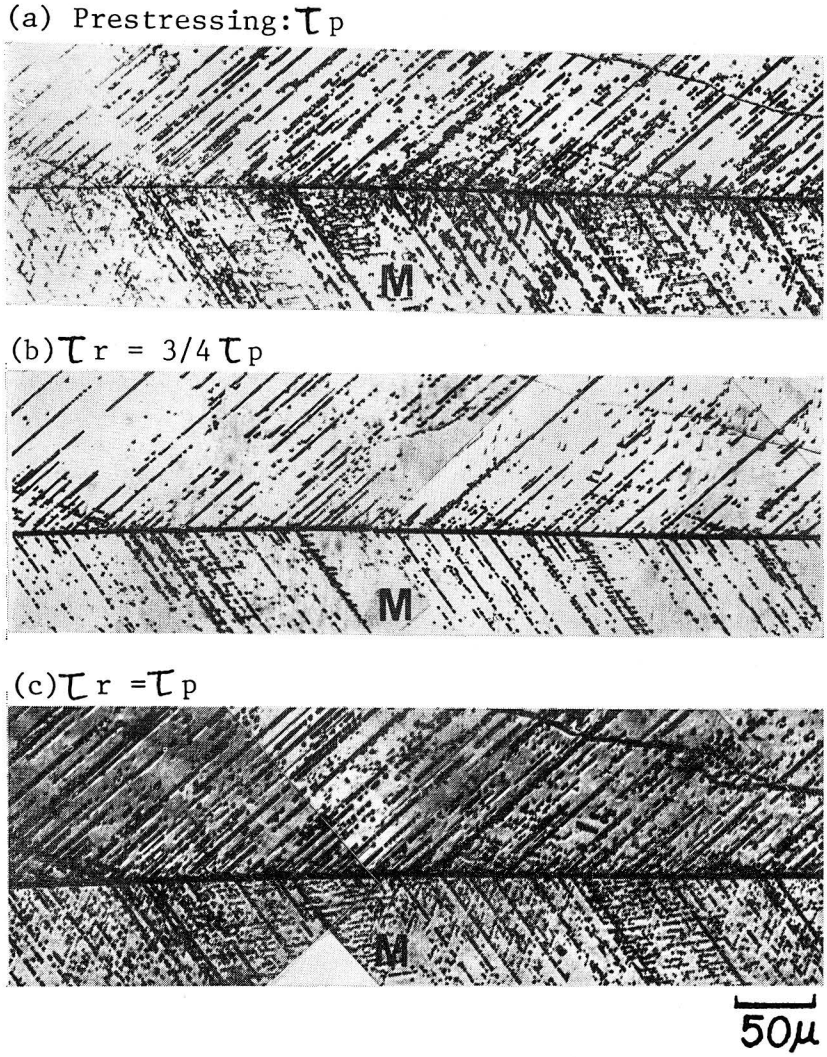

Fig. 15. Change of dislocation distributions near the grain boundary during reverse stressings in specimen B1. Point M will serve as a reference point of indentical position.

Much better defined secondary slips, which may be induced by the strong primary slip bands of adjacent crystal, were observed, as can be seen in the figure. Next, the specimen was subjected to reverse stress of $3/4\tau_p$. Dislocation distributions of this state are shown in Fig. 17. Secondary dislocations at the boundary decreased in density, and the contours of those diffused, though no significant change in the feature of long primary slip bands was observed. The results were similar to those for specimen B1.

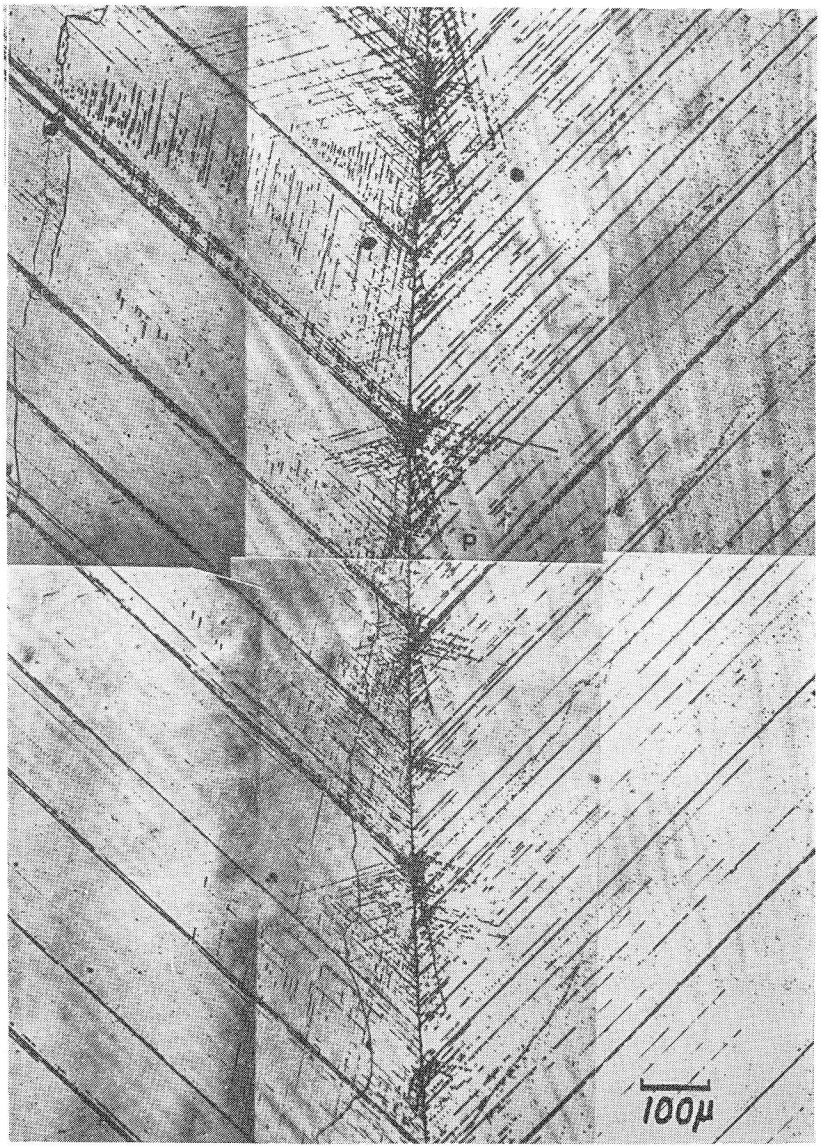

Fig. 16. Dislocation distributions near the grain boundary just past yielding in specimen B3. Point P will serve as a reference point of identical position in this and the next figure.

From the present results of both specimens, the predominant change near the boundary is ascribed to the large back stress at the grain boundary due to the large development of work hardening compared to that in the center of the crystal. The reason is that the dislocations near the boundary are able to move reversely much more than those in the center, through the aid of a high back stress, even though

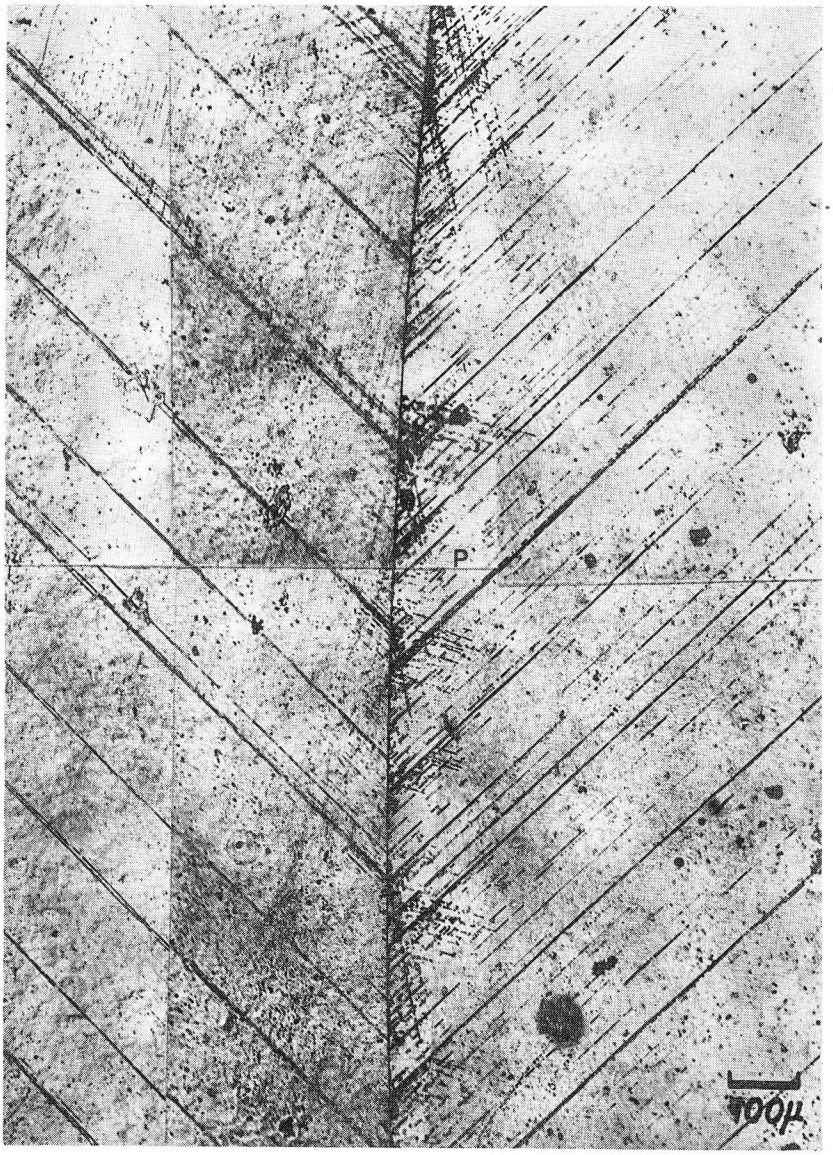

Fig. 17. Change of dislocation distributions near the grain boundary after reverse straining of $\tau_r = 3/4 \cdot \tau_p$ in specimen B3.

a small shear stress is applied. An estimation of the back stress will be represented in the following section 4. 3.

4. Discussion

4.1 Activation of secondary slip at grain boundary

4.1.1. Plastic strain compatibility (Macroscopic considerations)

The compatibility requirements for a bicrystal whose boundary is parallel to the stress axis have been discussed by Livingston and Chalmers[15], Hauser and Chalmers[16], and Kocks[18]. The treatment is reproduced here as follows.

Consider the bicrystal described in Fig. 18, with the three orthogonal axes x, y, z, such that y is normal to the grain boundary, x is in the boundary and z is the axis of the specimen, but not necessarily the tension axis. It will be assumed that the component single crystals A and B are oriented in such a manner that the resolved shear stress is greater on one slip plane than on the other. The deformation of the bicrystal can be described in terms of the six strain components; ε_{xx}, ε_{yy}, ε_{zz}, ε_{xy}, ε_{yz} and ε_{zx}. The stress situation will not be considered for the moment. If rectangular crystal A shears by an amount s_1^A on its primary slip system, then the three strain components of importance at the grain boundary are related to s_1^A as follows;

$$\varepsilon_{zz}^A = m_1^A s_1^A, \quad \varepsilon_{xx}^A = n_1^A s_1^A, \quad \varepsilon_{zx}^A = p_1^A s_1^A. \tag{1}$$

If e is a unit vector normal to the slip plane, and g a unit vector parallel to the slip direction, the three geometrical factors m_1^A, n_1^A, p_1^A, are defined by the following

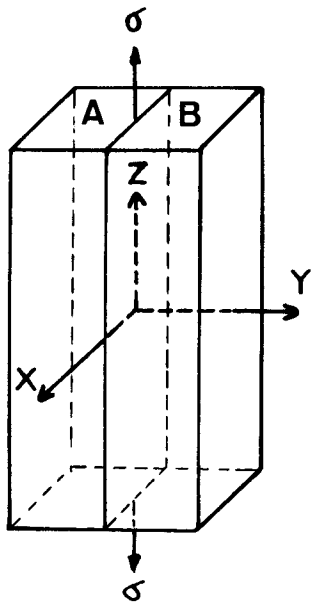

Fig. 18. A bicrystal with the grain doundary narmal to the X axis, and separating crystal A and B.

relations,

$$m_1^A=(z\cdot e)(z\cdot g),\quad n_1^A=(x\cdot e)(x\cdot g)$$
$$p_1^A=\frac{1}{2}[(z\cdot e)(x\cdot g)+(x\cdot e)(z\cdot g)], \tag{2}$$

where z for example, represents a unit vector along the z axis.

If we now consider crystals A and B deforming together as a bicrystal, i. e. if the boundary is not to slide or open up during deformation, we recognize that a continuity of material at the grain boundary must be maintained. Therefore, the compatibility conditions that must be satisfied at the boundary can be presented by the relations;

$$\varepsilon_{zz}^A=\varepsilon_{zz}^B,\quad \varepsilon_{xx}^A=\varepsilon_{xx}^B,\quad \varepsilon_{xz}^A=\varepsilon_{xz}^B. \tag{3}$$

If crystal B deforms by a small amount s_1^B on its primary slip system, a relation similar to expression (1) can be written for crystal B. Substituting (1) and the similar expression for B into relation (3) yields

$$m_1^A=cm_1^B,\quad n_1^A=cn_1^B,\quad p_1^A=cp_1^B, \tag{4}$$

where $c=s_1^B/s_1^A$. For any isoaxial bicrystal having the tensile axis whichis along the z axis, $m_1^A=m_1^B$. Hence, the crystals of an isoaxial bicrystal can slip on their primary slip systems alone and still satisfy the macroscopic continuity requirements only if $c=1$. Although the general isoaxial bicrystals, will not satisfy conditions (4), the requirements will be satisfied by all symmetric bicrystals. That is to say, for the symmetric bicrystal employed in the present experiments, one slip system in each component crystal suffices to fulfill the relation (3). For a bicrystal which does not satisfy these relations, the continuity requirements (3) will require the operation of slip systems in addition to the primary systems. As expression (3) represents three independent relations, and in addition there exists a fourth relation fixing the value of ε_{zz}, for an isoaxial non-symmetric bicrystal, the four independent conditions will be satisfied if slip on the primary slip system of one crystal is accompanied by slip on three slip systems of the second crystal. Tow slip systems in each crystal would also provide the necessary continuity requirements.

The isoaxial symmetric bicrystal, in which the single crystal A is a mirror image of the single crystal B with respect to the grain boundary, is elastically compatible. Therefore, the problem of elastic anisotropy due to the difference of elastic moduli will not be important in the elastic strain range.

The above analysis is based on the approximation that slip can be regarded as homogeneous shear deformation. Microscopic inhomogeneities that can develop at a grain boundary ignored in the compatibility treatments. All observations of dislocation distributions at the grain boundaries of the bicrystals employed in this experiment indicate that secondary slips and do occur even after a small straining just past yielding in spite of an isoaxial symmetric bicrystal. An αCu-Al alloy single

crystal of highly by concentrated aluminium oriented for a single slip, deforms less homogeneously, and the nature of the slip is characterized by a slip band or the so-called Lüders band. Hence, the requirements of macroscopic plastic compatibility are not satisfied sufficiently in the areas around the grain boundary where the primary slip is not symmetric with respect to the grain boundary. It is concluded that some parts of secondary slips activated at the grain boundary are caused by this microscopic incompatibility. The argument will be appreciated from the results that only for the bicrystal, much more narrow slip bands, compared with those for a single crystal, were generated simultaneously at yielding. These were distributed uniformly in the entire region of the gauge length which may be attributed to the requirements of continuity at the grain boundary.

The difference in the yield stress observed between single and bi-crystals may be associated with the lesser continuity of primary slip bands, and also to the different nature of formation of primary slip bands at yielding.

4.1.2 Stress concentration due to piled-up dislocations

Another type of microscopic incompatibility will result from the stress concentration ahead of primary dislocation pile-ups which must raise the resolved shear stress on the secondary slip systems of adjacent crystal above the critical resolved shear stress. Thus, the dislocation pile-ups which will be responsible for a secondary slip system activation are of interest from the view point of microscopic incompatibility in bicrystal.

The deformation of crystal A makes the adjacent crystal B shear on its primary slip system (Fig. 19). The shear in component crystal B induced by the primary slip in A can be resolved into all slip systems in B. The resultant shear stress P_i on slip system i (e_i, g_i) in B will be

$$P_i = P_A \cdot N_{A-i} = P_A[(e_A \cdot e_i)(g_A \cdot g_i) + (e_A \cdot g_i)(e_i \cdot g_A)], \tag{5}$$

where P_A is the effective shear stress on the primary slip system (e_A, g_A) in A, and N_{A-i} is the stress transforming factor[15,16]. Postulating that when the sum total of P_i and the applied resolved shear stress on the slip system i, τ_i^{ap}, arrives at the critical resolved shear stress, τ_c, the slip system i in B will be generated. Therefore, we obtain

$$\tau_c = P_i + \tau_i^{ap} = P_A \cdot N_{A-i} + \tau_i^{ap}, \tag{6}$$

or in terms of P_A,

$$P_A = (\tau_c - \tau_i^{ap}) \frac{1}{N_{A-i}} \tag{7}$$

Here, P_A, which will arise from the dislocation pile-ups at the grain boundary is most important, because the stress near the boundary can attain a high value close to the spearhead of the pile-up. P_A will depend on the length of the pile-up and

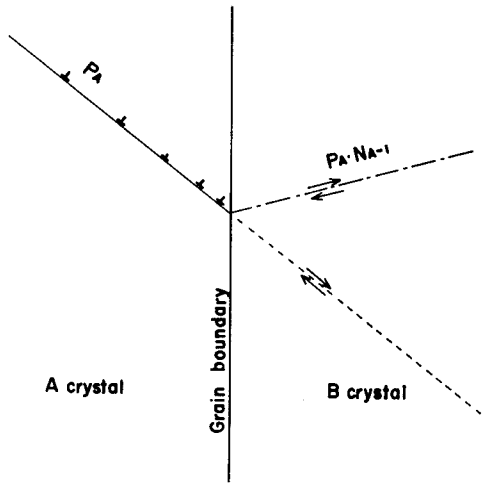

Fig. 19. Dislocation pile-ups at a grain boundary. P_A is the effective shear stress on the primary slip system in a crystal. N_{A-i} is the stress transforming factor.

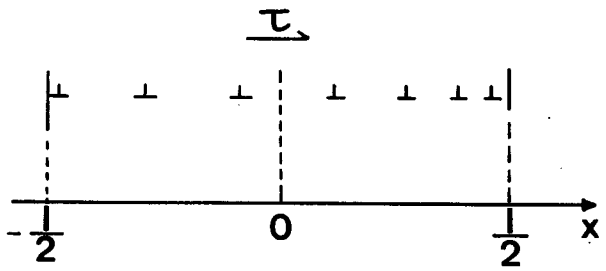

Fig. 20. Single pile-up of edge dislocations.

the distance between the area ahead of the pile-up and the dislocation source of slip system i in B, which be generated by the stress concentration of the pile-up. An analysis of the pile-up which initiates yielding on the other side of the grain boundary will be given as follows.

The stress distribution resulting from an isolated pile-up has been essentially given with the continuous-dislocation model by Eshelby et al. [19] A pile up of N edge dislocations of Burgers vector b is formed in front of an obstalce such a grain boundary in the presence of an effectively resolved external shear stress τ, as shown in Fig. 20. Dislocation distribution in the single pile-up of length ℓ is

$$n(x)=\frac{2(1-\nu)\tau}{\mu b}\left(\frac{\frac{\ell}{2}+x}{\frac{\ell}{2}-x}\right)^{1/2}, \tag{8}$$

where μ is shear modulus and ν Poisson's ratio. The total number of dislocations in the distribution is given by

$$N=\int_{-\ell/2}^{\ell/2} n(x)dx=\frac{\pi(1-\nu)\tau\ell}{\mu b} \tag{9}$$

The stress τ_I developed by the pile-up in its neighbourhood is deduced from the knowledge of the back stress produced by the pile-up, and yielding the results[20],

$$\tau_I=\tau\left\{\left(\frac{x+\frac{\ell}{2}}{x-\frac{\ell}{2}}\right)^{1/2}-1\right\}. \tag{10}$$

At large distances, the pile-up exerts the same stress as a single dislocation of Burgers vector Nb,

$$\tau_I\cong\frac{\mu Nb}{2\pi(1-\nu)x},\quad x\gg\frac{\ell}{2}. \tag{11}$$

Near the spearhead of the pile-up, where $x-\ell/2\ll\ell/2$

$$\tau_I\cong\tau\left(\frac{\ell}{x-\frac{\ell}{2}}\right)^{1/2}=\tau\alpha. \tag{12}$$

The stress concentration factor α is $(\ell/r)^{1/2}$, where the distance from the tip $r\equiv x-\ell/2$. The stresses can attain rather high values close to the spearhead. Consequently, the results of the continuous distribution solution cannot be used to obtain the stress concentration at the tip of the pile-up, i. e. at distances closer than the separation between the leading dislocations.

We now consider an isolated pile-up which promotes the activation of an adjacent dislocation source. The values of the stress transforming factors N_{A-i} on twelve active slip systems are represented in Table 2. The values of P_i and $P_i+\tau_i^{ap}$ when the resolved shear stress of the critical slip system (111) $[10\bar{1}]$ reaches the critical shear stress, $\tau_c\cong 1.1$ kg/mm^2, are also represented in the table, since the value $P_i+\tau_i^{ap}$

Table 2. Schmid factor, N_{A-i}, P_i and $P_i+\tau_i^{ap}$ for active slip systems.

Slip system			Schmid factor	N_{A-i}	P_i(kg/mm^2)	$P_i+\tau_i^{ap}$ (kg/mm^2)
Primary	$(11\bar{1})$	$[1\bar{1}0]$	0.107	0.756	0.255	0.505
		$[101]$	0.471	0.886	0.299	1.399
		$[011]$	0.401	0.685	0.029	0.965
Conjugate	$(1\bar{1}1)$	$[110]$	0.235	0.988	0.333	0.882
		$[10\bar{1}]$	0.106	0.639	0.215	0.463
		$[011]$	0.142	0.282	0.095	0.427
Critical	(111)	$[1\bar{1}0]$	0.142	0.555	0.187	0.519
		$[10\bar{1}]$	0.397	0.514	0.173	1.100
		$[0\bar{1}1]$	0.250	0.787	0.265	0.849
Cross slip	$(1\bar{1}\bar{1})$	$[110]$	——	0.281	0.095	0.095
		$[101]$	——	0.291	0.098	0.098
		$[0\bar{1}1]$	——	0.013	0.004	0.004

of the critical slip system is the greatest among other secondary slip systems. In this condition, for the critical slip system, we obtain the effective shear stress on the primary slip system P_A to be 0.337 kg/mm² by Eq. (7)

Although an adequate estimation of ℓ and r is somewhat difficult from the present etch pit observations, assuming that $\ell=100\mu$ and $r=10\mu$, Eq. (12) gives the stress concentration factor α to be 3.16. Therefore, the minimum shear stress τ to initiate yielding in the slip system is to be P_A/α (kg/mm²), because the stress τ_I developed by the pile-up in its neighbourhood is considered to be equivalent to P_A. Consequently, substituting the values of $\mu=4.2\times10^3$kg/mm², $\nu=0.33$ and $b=2.6\times10^{-7}$ mm for the Cu-Al alloy, and $\ell=0.1$ mm and $\tau=0.11$ kg/mm² into Eq. (9), the following estimate for the total number of disloctions in such a pile-up yields

$$N=\frac{\pi(1-\nu)\ell\tau}{\mu b}=20. \tag{13}$$

It should be noted that the value of N from the present analysis is based on the stress distribution of a simple isolated pile-up, and neglects interaction stress between other dislocation groups located nearby. However, many additional short dislocations, which were generated by the pile-up approximately equivalent to the computed result, were observable in Figs 6, 15 or 16. This estimation is thus considered to be reasonable.

Again, from the results of $P_i+\tau_i^{ap}$ in Table 2, the primary slip systems $(11\bar{1})$ [101] and $(11\bar{1})$ [011] can attain a higher value. Also, the value of the conjugate slip system $(1\bar{1}1)$ [110] is comparable to that of these systems. Short rows of pits of primary and secondary slip systems in adjacent crystals and much higher etch-pit density zones which were formed along the direction of primary slip of adjacent crystal, (Figs. 6 (c) and 8 (b)), indicate that the high stress concentration near the tip of a pile-up plays an important role in promoting additional slips on the other side of the crystal.

4.2 Strength of grain boundary

It is evident that a multiple slip occurred in the grain boundary vicinity in the early stage of deformation, and then the slip developed with an increasing strain, as is indicated in Fig. 7 or 8. The multiple slip must provide the observed differences in flow stress and in the rate of work hardening between single crystals and the corresponding bicrystals. The magnitude of the differences will depend on the volume fraction of the grain boundary deformation zone (multiple slip layer) to the entire volume of bulk, and the degree of intensity in the zone. Hence, it is important to evaluate the true strength in the grain boundary vicinity where large interaction stresses act on dislocations.

If a clearly defined zone of a multiple slip in the grain boundary vicinity exists

in a bicrystal, the difference in flow stress, $\Delta\sigma$, required to produce a given strain will be written as

$$\Delta\sigma=\sigma_B-\sigma_S=V_{GB}(\bar{\sigma}_{GB}-\sigma_S), \tag{14}$$

where σ_B, σ_S is the applied stress of bicrystal and component single crystal respectively, V_{GB} is the volume fraction of the multiple slip layer and $\bar{\sigma}_{GB}$ is the average stress in the multiple slip layer. In the early stage of deformation, the zone was located inhomogeneously. (See for example Figs. 7 (a), 16.) However, it appears that, with an increasing strain, the multiple slip layer existed rather uniformly, as indicated in Fig. 8 (b).

As an example, based on the data of flow stresses in specimen B4 and S7 and the etch-pit observations, the average grain boundary strength, $\bar{\sigma}_{GB}$, can be obtained as follows. It was shown in Fig. 4 that $\sigma_B=2.78\,\mathrm{kg/mm^2}$, $\sigma_S=2.53\,\mathrm{kg/mm^2}$ at the strain of 3%. But, considering the difference of yield stress between these crystals, the difference in flow stress $\Delta\sigma$ is consequently $0.1\,\mathrm{kg/mm^2}$. From the etch-pit results of Fig. 7 (c) or 8 (b), the multiple slip layer in each component single crystal was about 250 μ and the width of the component crystal was 3.5 mm. Hence, the volume fraction of the multiple slip layer V_{GB} is $V_{GB}=0.25\,\mathrm{mm}/3.5\,\mathrm{mm}=0.07$ in these circumstances. Therefore, substituting these values in Eq. (14), the value of $\bar{\sigma}_{GB}$ is calculated as

$$\bar{\sigma}_{GB}=\frac{\Delta\sigma}{V_{GB}}+\sigma_S=3.96\,\mathrm{kg/mm^2}. \tag{15}$$

The flow stress for the grain boundary deformation zone from the present calculation is approximately one and a half times larger than that for the component single crystal. The stress is equivalent to the flow stress of a single crystal extended to the early stage of Stage II of the work-hardening curve. It is concluded that the calculated result is consistent with the observations that many secondary dislocations interact with primary dislocations in the high etch-pit density zone near the boundary. Hence, it becomes possible that the average strength of a grain boundary deformation zone can be evaluated strictly with the aid of direct observation of dislocation distributions near the boundary.

4.3 The Bauschinger effect

It becomes evident that the predominant change of dislocation distributions took place near the boundary during reverse loading, as mentioned in section 3.2.2. This must be attributed to the higher back stress at the boundary compared with that of the center of the crystal. An applied stress, τ_1, is generally represented by the sum of the dislocation frictional stress, τ_f, and the elastic interaction stress, τ_G. Therefore, the external stress, τ_2, at which the first dislocation movement in backward direction occurs, yields the following relation,

$$\tau_2=\tau_G-\tau_f. \tag{16}$$

The back stress acts on dislocation in the same way as the elastic stress, τ_G, by the definition of the problem. The frictional stress, τ_f, is considered to be independent of the magnitude of an applied stress because the stress is an intrinsic stress of a metal which forces a dislocation line to slip. Therefore, the higher the elastic stress, the more dislocation can move backward even when a small unloading or reverse stress takes place. It has been pointed out that, near the grain boundary, multiple slip occurs actively, probably due to a high stress concentration of pile-up of adjacent crystal and microscopic incompatibility. Thus, the average back stress at the grain boundary is somewhat higher than in the center of the crystal because the work hardening rate in the boundary deformation zone (multiple slip layer) is greater than that in the center, as shown in the previous section 4. 2.

Another factor providing a high back stress is ascribed to high density dislocation pile-ups at the grain boundary. Knowledge of the back stress, τ_B, produced by the pile-up which was shown in Fig. 20 has been given by Hirth and Lothe[20] as the relation

$$\tau_B=-\tau\left\{1-\left(\frac{x+\frac{\ell}{2}}{x-\frac{\ell}{2}}\right)^{1/2}\right\}, \quad x<-\frac{\ell}{2}. \tag{17}$$

At $x=-\ell/2$, $\tau_B=-\tau$, by definition of the problem, is the correct value of the back stress in the interval $-\ell/2<x<\ell/2$. Asymptotically, for $x\ll-\ell/2$, τ_B reduces to

$$\tau_B=\frac{\mu Nb}{2\pi(1-\nu)x}, \tag{18}$$

which is the back stress from a super-dislocation Nb. Therefore, if x is fixed, the back stress, τ_B, is in proportion to N and, in a region far from the dislocation dense-aligned zone, τ_B reduces to a small value.

Based on the argument of back stress, the dislocations near the boundary will be able to move backward at a smaller reverse stress than those in the center region. However, the mean free paths of these dislocations will be rather small, since at the boundary multiple slip occurs actively. Hence the dislocations cannot move backwards easily because of the interference of secondary dislocations. The estimation of the magnitude of this interference effect, compared with the simple primary slip zone which is almost equivalent to the case of single crystal, is very difficult. However, from a simple model indicated in Fig. 12, it can be seen that the average magnitude of the back motion of dislocations is suppressed when the secondary dislocations act as a barrier of back motion. That is to say, the Bauschinger strain produced by the sum of the distance of back motion of individual dislocations must be smaller than that single crystal. The argument is consistent with the results of

Buckley and Entwistle[4], that in single crystals, the stressing in Stage I results in large Bauschinger strains which are proportional to the amount of pre-stain and do not increase significantly in Stage II. The grain-size dependence of the Bauschinger effect which was pointed out by Gokyu et al.[5] cannot be explained from the present observations and deductions.

5. Conclusions

An etch pitting technique was used to study the dislocation distributions in deformed Cu-9 at.% Al isoaxial symmetric bicrystals, in which a component crystal is the mirror image of the crystal on the other side with respect to the grain boundary and oriented for single slip $(11\bar{1})$ [101]. In order to investigate the contribution of the grain boundary to the Bauschinger effect, the dislocation behaviour near the boundary region when the specimens were subjected to reverse stress, was also studied. The following conclusions were drawn.

1) Although the bicrystal deforms on two slip systems, one system in each single crystal, from the view point of macroscopic plastic compatibility, secondary slips and short primary slips were activated neart the boundary region even by a small strain just past yielding, and this boundary slip zone developed with increasing strain. It is concluded that most of the slips were induced by the stress concentration due to pile-up dislocations of the primary slip system of the adjacent crystal. Some of them can be explained by microscopic incompatibility, due to the mismatch of primary slip bands in each component crystal at the boundary.

2) In the bicrystal, many primary slip bands whose width was far narrower than that for single crystal were activated rather uniformly in the entire region of the gauge length. This occurrence may be attributed to the requirements of macroscopic continuity of the grain boundary region.

3) The average strength of latent hardening in the grain boundary slip zone (multiple slip layer) at a given strain was estimated from the measured values of applied stresses for single and bi-crystal and of the volume fraction of the grain boundary slip zone. The results were equivalent to the stress deduced from the etch-pit density of this slip zone.

4) The induced secondary dislocations between primary slip bands near the boundary were unstable against reverse loading, except for the region of "cross-point" with primary dislocations. In the first stage prior to reaching a full reverse stress, most of these dislocations were annihilated and then recovered by a further reverse stress. This behaviour is closely connected with a weakening near the grain boundary region during reverse stress.

5) Dislocations near the boundary can move even a small reverse stress back-

wards by the aid of a high back stress on dislocations, because of the latent hardening by multiple slip and piled-up dislocations. However, the mean free path of these dislocations is found to be small, due to the interference of secondary dislocations. It is concluded that the Bauschinger effect in the multiple slip layer is smaller than that in the center of crystal.

References

1) G. Sachs and H. Shoji; Z. Phys., **45**, 776 (1927).
2) E. Heyn and Banel; Met. und Erz., **15**, 411 (1918).
3) G. Masing; Wiss Ver Siemens-Konz., **3**, 231 (1923).
4) S. N. Buckley and K. M. Entwistle; Acta Met., **4**, 352 (1956).
5) I. Gokyu, T. Kishi and H. Wada; J. Japan Inst. Metals, **31**, 154 (1970).
6) J. Takamura and S. Miura; J. Phys. Soc. Japan, **13**, 1421 (1958).
7) See a review work, J. P. Hirth; Met. Trans., **3**, 3047 (1972).
8) R. E. Hook and J. P. Hirth; Acta Met., **15**, 535 (1967).
9) R. E. Hook and J. P. Hirth; Ibid., **15**, 1099 (1967).
10) R. E. Hook and J. P. Hirth; Trans. Japan Inst. Metals, Suppl. vol. **9**, p. 778 (1968).
11) F. W. Young, Jr.; J. Appl. Phys., **32**, 192 (1961).
12) J. D. Livingston; J. Appl. Phys., **31**, 1071 (1960).
13) F. W. Young, Jr.; J. Appl. Phys., **32**, 3553 (1961).
14) F. W. Young, Jr.; J. Appl. Phys., **33**, 3553 (1962).
15) J. D. Livingston and B. Chalmers; Acta Met., **5**, 322 (1957).
16) J. J. Hauser and B. Chalmers; Acta Met., **9**, 802 (1961).
17) J. D. Livingston; Direct Observations of Imperfections in crystal, Interscience, New York, p. 116 (1962).
18) U. F. Kocks; Phil. Mag., **10**, 187 (1964).
19) J. D. Eshelby, F. C. Frank and F. R. N. Nabarro; Phil. Mag., **42**, 351 (1951).
20) J. P. Hirth and J. Lothe; "Theory of Dislocations", McGraw-Hill, New York, p. 694 (1968).